Chemical Science

ROYAL SOCIETY OF CHEMISTRY

EDGE ARTICLE

View Article Online
View Journal | View Issue

Cite this: *Chem. Sci.*, 2025, **16**, 23321

All publication charges for this article have been paid for by the Royal Society of Chemistry

Received 26th June 2025
Accepted 29th October 2025

DOI: 10.1039/d5sc04710b

rsc.li/chemical-science

Compositional selection of phospholipid compartments in icy environments drives the enrichment of encapsulated genetic information

Tatsuya Shinoda,[a] Natsumi Noda,[b] Takayoshi Watanabe,[bc] Kazumu Kaneko,[d] Yasuhito Sekine[b] and Tomoaki Matsuura *[b]

The lipid world hypothesis proposes that both intracellular components and the chemical composition of the membrane compartment can act as heritable information, contributing to protocellular fitness. However, there are few experimental demonstrations of membrane compositional selection, and none of them have expanded to the associated transfer of encapsulated contents, representing a possible early form of inheritance. Here, we quantitatively demonstrated that the growth of phospholipid vesicles depends on their lipid composition under freezing and thawing (F/T) cycling: vesicles with more unsaturated bonds in the acyl chain showed higher growth, membrane mixing, and content mixing efficiencies. When vesicles composed of phospholipids with either one or two unsaturated bonds were mixed and subjected to F/T cycles, a selective enrichment of the lipid with two unsaturated bonds was observed in the grown vesicles. Moreover, selection acting on lipid composition was propagated to the encapsulated genetic material, which was also enriched, while it did not play a particular role and thus was selectively neutral. We conclude that membrane lipid composition can be a direct target of selection for grown vesicles under an icy environment, leading to indirect but concurrent enrichment of compartmentalized genetic molecules—independent of their encoded information.

Introduction

Compartmentalization was likely a key factor for the origin of life. With distinct compartments that shield internal chemical components and their reactions from the external environment,[1,2] primordial cells could diversify and compete, leading to early Darwinian evolution.[3] Experimental studies support this view, demonstrating that diversity among encapsulated systems can induce competition among protocells.[4–6] The lipid world hypothesis, however, argues that both the encapsulated systems and the membrane compartment itself carry heritable information and contribute to protocellular fitness[7] – a perspective that emphasizes the importance of the membrane and its composition. Indeed, simulations using the graded autocatalysis replication domain (GARD) model suggest that lipid assemblies can store and transmit their lipid compositions as heritable information, allowing specific compositions to adapt to environmental pressure.[8–10] Building upon these theoretical insights, compositional selection has been experimentally demonstrated with oil droplets[11] and phospholipid-fatty acid mixed membranes.[12–14] Although oil droplets and fatty acid vesicles offer certain advantages in a prebiotic context due to their simplicity and plausibility,[15] a high permeability to biomolecules, protons, and other ions,[16,17] limits their ability to store compartmentalized metabolites and diminishes their relevance as effective models of a primordial cell. In contrast, phospholipid membranes exhibit an enhanced capacity for retaining compartmentalized contents,[16–18] and could be synthesized under prebiotic conditions.[19–21] Therefore, it is possible that protocells were made of phospholipids, while it is unclear if compositional selection could occur with these compartments.

As compartments generally grow in size before fission, the growth of a compartment is likely a prerequisite for the proliferation of protocellular systems,[22] and a fast growth rate within a certain environment would be a selective advantage for the protocell. While contemporary cells use sophisticated molecular machinery for compartment growth, various growing mechanisms for primordial cells have been proposed, including uptake of lipid molecules or micelles,[23,24] vesicle fusion[25,26] and even *in situ* synthesis of amphiphiles.[20,27] Among them, vesicle fusion induced by freeze–thaw (F/T) cycles[28] has been a prebiotically plausible and thus an attractive strategy for its contents transferring capacity and more importantly due to the universal potential for temperature cycling on early Earth[29] and other

[a]*Department of Life Science and Technology, Institute of Science Tokyo, 152-8550, Japan*
[b]*Earth-Life Science Institute (ELSI), Institute of Science Tokyo, Tokyo 152-8550, Japan. E-mail: matsuura_tomoaki@elsi.jp*
[c]*MAQsys Inc., Kanagawa 213-0012, Japan*
[d]*Department of Earth and Planetary Sciences, Institute of Science Tokyo, Tokyo 152-8550, Japan*

planetary bodies like icy moons.[30] If phospholipid composition contributes to protocellular fitness, a selective enrichment of specific phospholipid compositions in the vesicle "offspring" should be detectable. Likewise, the encapsulated molecules, including metabolites and genetic information, should also be enriched even if they do not play a particular role and thus are selectively neutral. This could be representing a possible primitive form of inheritance. This inheritance is governed by the selection based on the physicochemical properties of compartments and the direct transfer of their components, in contrast to canonical genetic inheritance, where gene-encoded functions play the major roles. Yet, no experimental demonstration of such selection dynamics in phospholipid vesicles has been reported.

In this study, we experimentally explored phospholipid-dependent vesicle growth within an icy environment undergoing cycles of F/T. We found that vesicles with different lipid compositions do exhibit variation in growth rate under F/T conditions (Fig. 1A). When vesicles with different lipid compositions were mixed, F/T induced a selective partitioning of the phospholipid with more unsaturated bonds (Fig. 1B). Finally, we found that the F/T-induced selection for growth-prone phospholipid led to the co-enrichment of their compartmentalized genetic molecules, even though these materials were not playing a particular role and thus selectively neutral (Fig. 1C). This study is the first to demonstrate the selection of phospholipid composition and accompanied enrichment of compartmentalized genetic molecules in an icy environment, a prebiotically plausible environment that can trigger the growth of protocells.

Results and discussion

F/T cycles induce phospholipid-dependent vesicle fusion

We first investigated whether vesicles subjected to F/T conditions show variable degrees of growth depending on lipid compositions (Fig. 1A). Large unilamellar vesicles (LUVs) with four different lipid compositions, *i.e.*, (i) 100% POPC, (ii) 80% POPC: 20% PLPC, (iii) 50% POPC: 50% PLPC, and (iv) 100% PLPC, were prepared (Fig. 1D). The initial vesicle size (~100 nm in diameter) was confirmed by dynamic light scattering (DLS) analysis and transmission electron microscopy (TEM) (Fig. 2A, top; Fig. 2B, top). To increase fusion efficiency during F/T, vesicles were pelleted using an ultracentrifuge (630 000 g for 30 min at 4 °C; hereafter, the term "pellet" refers to ultracentrifugation under these conditions), bringing the vesicles into proximity with each other. F/T was performed by freezing vesicles in liquid nitrogen for 1 min and then thawing at room temperature (~24 °C) for around 10 min until the ice completely melted. The thawed sample was vortexed prior to pelleting for subsequent F/T cycles (Fig. 2C). After repeating F/T three times (denoted as 3 × F/T cycles hereafter), DLS measurements showed new peaks with vesicle diameters increase by one or more orders of magnitude compared to the original diameter for all phospholipid compositions tested (Fig. 2A, bottom). Consistently, TEM observations also revealed enlarged and fused vesicles after 3 × F/T cycles (Fig. 2B, bottom). The POPC samples frequently showed multiple vesicles aggregate with apparent interfaces, whereas PLPC samples exhibited large vesicles (several to 10 micrometers in size) with no interfaces, indicating the mixing of the lipid molecules from different vesicles (Fig. 2B and S1). These TEM images were consistent with the results from the membrane mixing experiments described below (Fig. 3). Note that peaks corresponding to fused growth were not observed for the samples without F/T or with F/T but without pelleting (Fig. S2).

To assess the proportion of vesicles that grew, centrifugal separation at 20 000 g for 30 min at 4 °C was performed on the vesicles after F/T cycles. The precipitated vesicles collected from this process were designated as "grown vesicles", while

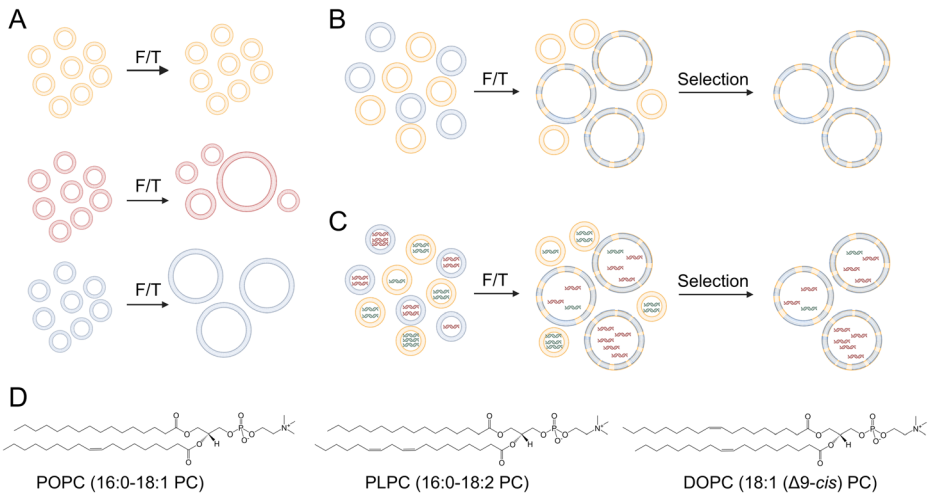

Fig. 1 Schematics of freeze–thaw (F/T) cycles applied to vesicles composed of different phospholipids. (A) Examples of F/T with three different phospholipid compositions. Fusion occurs more efficiently in the order of blue, red, and orange vesicles. (B) F/T of a mixture of two different vesicles. The blue lipid is preferentially recruited into growing vesicles. (C) F/T of a mixture of two vesicles with different compositions of lipid. The encapsulated DNA is different but selectively neutral. (D) Chemical structures of the phospholipids used in this study: 1-palmitoyl-2-oleoyl-*glycero*-3-phosphocholine (POPC, 16 : 0–18 : 1 PC), 1-palmitoyl-2-linoleoyl-*sn-glycero*-3-phosphocholine (PLPC, 16 : 0–18 : 2 PC), 1,2-di-oleoyl-*sn-glycero*-3-phosphocholine (DOPC, 18 : 1 (Δ9-Cis) PC).

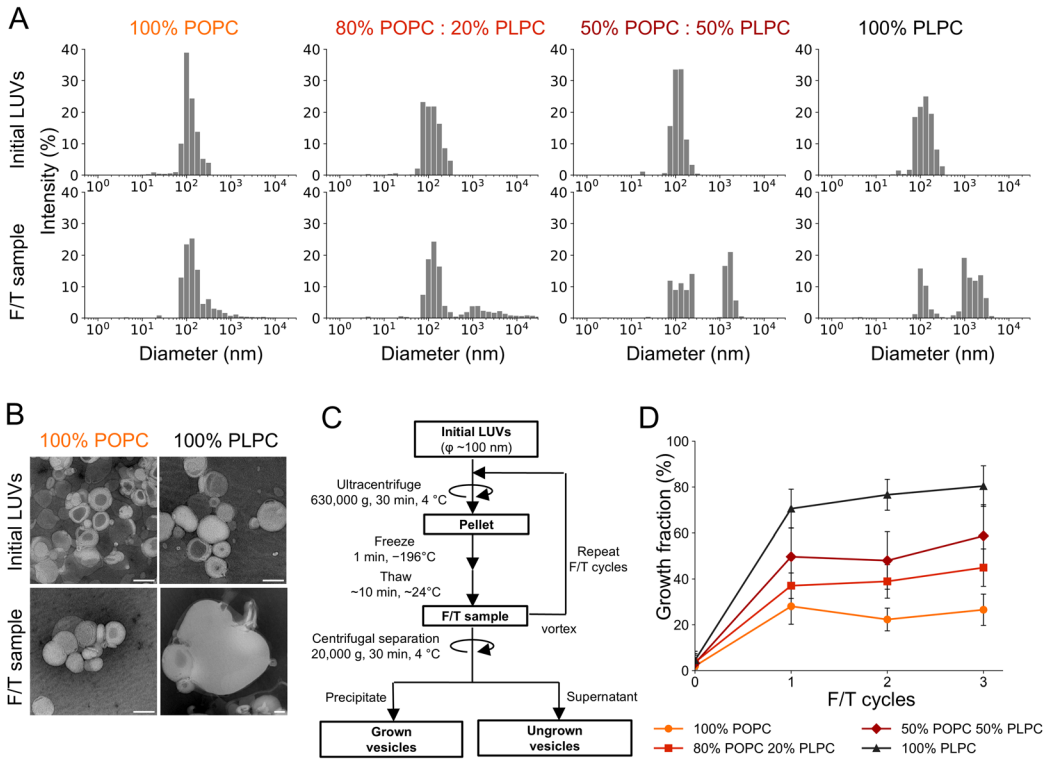

Fig. 2 The F/T-induced growth of vesicles with four different initial phospholipid compositions. (A) Size distribution obtained using DLS measurements. The top panels show the results for initial LUVs while the bottom panels show the results after 3 × F/T cycles. (B) TEM images of 100% POPC and 100% PLPC vesicles before and after 3 × F/T cycles. Scale bars 100 nm. (C) Flowchart showing the F/T experimental procedure used in the present study. The ultracentrifuged LUV pellet was subjected to F/T followed by vortexing. Grown and ungrown vesicles were distinguished by centrifugal separation. (D) Growth fraction as a function of the number of F/T cycles. Each error bar represents the standard deviation calculated from three independent experiments ($n = 3$).

"ungrown vesicles" refers to the vesicles that remained in the supernatant (Fig. 2C). We confirmed through DLS measurements that "ungrown vesicles" predominantly centered around their initial diameter of 100 nm, whereas "grown vesicles" showed a distinct shift toward larger sizes (Fig. S3). Using an enzymatic lipid quantification assay, we defined growth fraction

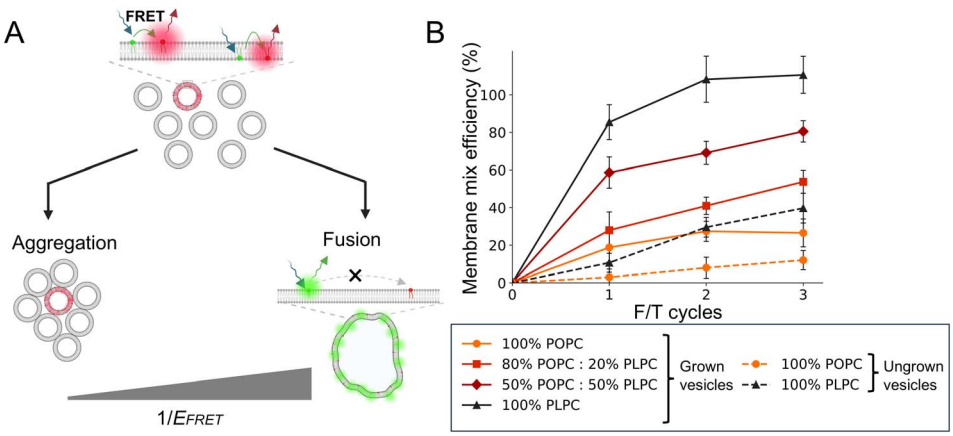

Fig. 3 Membrane mixing of F/T-induced grown vesicles. (A) Schematic illustrating the FRET assay to quantify and distinguish two possible mechanisms for vesicle growth: vesicle aggregation (bottom left) and vesicle fusion (bottom right). The reciprocal of FRET efficiency, $1/E_{FRET}$, is expected to increase with the distance between the fluorescent donor, NBD (green dots), and the acceptor, rhodamine (red dots). (B) Membrane mix efficiencies of grown (solid lines) and ungrown (broken lines) vesicles after 1–3 × F/T cycles. Each error bar represents the standard deviation calculated from two independent experiments, each with three measurements ($n = 6$). 0% is defined as the $1/E_{FRET}$ value for the initial LUVs. 100% is defined as the $1/E_{FRET}$ value of LUVs containing both NBD-tagged and rhodamine-tagged lipids at a concentration assuming homogenous mixing of fluorescent: non-fluorescent LUV = 1 : 7 (Fig. S7B).

as the mass fraction of lipids of grown vesicles over the total (sum of grown and ungrown vesicles). The near-zero values of growth fraction without F/T (0 × F/T cycle in Fig. 2D) indicate that the centrifugal separation is mild enough to retain initial LUVs in the supernatant and does not remove the ungrown vesicles. In contrast, high growth fractions after 1–3 × F/T cycles in all phospholipid compositions (Fig. 2D) were consistent with our DLS analyses (Fig. 2A). The growth fraction increased with the fraction of PLPC in the initial composition: whereas 100% POPC (*i.e.*, 0% PLPC) had a growth fraction of 27 ± 7%, 100% PLPC (*i.e.*, 0% POPC) had a growth fraction of 78 ± 9% (Fig. 2D), with intermediate compositions have intermediate growth fractions. The one additional unsaturated bond in PLPC relative to POPC might have resulted in more destabilized lateral packing of the vesicle membrane, rendering vesicles with higher PLPC content more susceptible to fusion during F/T. In each case, the growth fraction is stable across successive rounds of F/T (Fig. 2D). When isolated ungrown vesicles were subjected to additional F/T cycling (Fig. S4 and S5), the growth fraction was low, suggesting the limited growth potential of the ungrown vesicles. The TEM images of ungrown vesicles showed that vesicles that are smaller than the initial ones (Fig. S1). It is possible that the small ones can no longer pellet by ultracentrifugation, resulting in the plateau of the overall growth fraction (Fig. 1D). See SI (Fig. S1, S4 and S5) for details.

Phospholipid-dependent membrane mixing during F/T-induced vesicle fusion

The grown vesicles after F/T cycles were sufficiently large for observation *via* laser scanning confocal microscopy (LSCM) (Fig. S6). When two LUV species with membranes containing fluorescently labeled lipids—one with nitrobenzoxadiazole (NBD)-tagged lipids and the other with rhodamine-tagged lipids—were mixed and subjected to 3 × F/T cycles, the grown vesicles exhibited overlapping fluorescence signals (Fig. S6), indicating that membrane mixing had occurred in the grown vesicles. However, because of the lack of resolution of LSCM, it is not possible to quantify the mixing of membrane lipids at the molecular level. We thus used fluorescence resonance energy transfer (FRET) to quantitatively assess the membrane mixing mechanism (Fig. 3A). As membrane mixing occurs, the distance between the two fluorophores increases, leading to a decrease in the FRET signal and an increase in the NBD fluorescence (Fig. 3A, right). Conversely, aggregation of LUVs results in little change in FRET signal (Fig. 3A, left). We prepared LUVs containing both NBD- and rhodamine-tagged lipids as fluorescence donor and acceptor, respectively, and mixed the labeled LUVs with LUVs without any fluorophores (1 : 7 mass ratio) and subjected them to F/T cycles. We then measured the fluorescence of rhodamine and NBD, and calculated the FRET efficiency, E_{FRET}, and used its reciprocal, $1/E_{FRET}$, as an indicator of the membrane mixing (Fig. 3A; see Materials and methods in SI); the larger the $1/E_{FRET}$ value is the more the membrane is mixed, and *vice versa*. We found that $1/E_{FRET}$ of grown vesicles increased after 1–3 × F/T cycles compared to that of the initial LUVs (0 × F/T cycle), irrespective of the initial phospholipid composition (Fig. S7A). Furthermore, $1/E_{FRET}$ after 3 × F/T cycles increased along the PLPC percentage (Fig. S7A), indicating that a higher PLPC content resulted in grown vesicles with membranes better mixed than those with lower PLPC content, consistent with the TEM images shown in Fig. 2B.

We then converted $1/E_{FRET}$ into membrane mix efficiencies (Fig. 3B; see Materials and methods in SI for details). Here, 0% corresponds to aggregation of LUVs (*i.e.*, no membrane mixing) (Fig. 3A, left) and 100% corresponds to homogenous mixing of lipids (Fig. 3A, right). After 2–3 × F/T cycles, the membrane mix efficiency approached nearly 100% for 100% PLPC vesicles, while it remained below 30% for 100% POPC (*i.e.,* 0% PLPC) vesicles. The first F/T cycle showed the most significant increase in the membrane mixing of grown vesicles compared to subsequent F/T cycles irrespective of phospholipid composition (Fig. 3B); this result mirrors that of the growth fraction (Fig. 2D), which also increased the most after the first F/T cycle. Note that values slightly exceeding 100% membrane mix efficiency of PLPC are likely due to a statistical error. In contrast to grown vesicles, low membrane mix efficiencies (up to 30%) of ungrown vesicles (Fig. 2C) were observed (Fig. 3B, broken lines), which suggests a positive correlation between membrane mixing and vesicle growth.

Phospholipid-dependent mixing of encapsulated materials as a result of F/T-induced vesicle fusion

Vesicle fusion may also result in mixing or leakage of internal contents. To explore whether grown vesicles incorporate and maintain the contents compartmentalized within the initial LUVs that fuse to form the grown vesicles, two populations of LUVs encapsulating two different molecules, a calcein–cobalt (Co^{2+}) complex and EDTA, respectively, were mixed at a 1 : 1 ratio and subjected to F/T cycles (Fig. 4A). Upon content mixing, EDTA chelates Co^{2+}, restoring calcein fluorescence that had been initially quenched by Co^{2+} (Fig. 4A), as observed by LSCM (Fig. 4B). We thus tracked calcein fluorescence across F/T cycles in the grown vesicles composed of four different phospholipid compositions (Fig. 4C). We confirmed that calcein fluorescence significantly increased after the first F/T cycle for all phospholipid compositions (Fig. 4C). After 3 × F/T cycles, we saw a clear trend where the higher the PLPC percentage was, the lower the fluorescence intensity of the resulting grown vesicles (Fig. 4C).

Note that the fluorescence change observed in Fig. 4C is an overlay of (i) content mixing and (ii) content leakage triggered by F/T. To quantify the influence of content leakage on the change in the fluorescence observed in Fig. 4C, LUVs encapsulating fluorescent calcein made of four different phospholipid compositions were subjected to F/T cycles. Content leakage in the form of fluorescence intensity loss was observed in all LUV compositions tested and showed a clear dependency on phospholipid composition (Fig. 4D). The higher the PLPC content, the greater the fluorescence intensity decrease, which we speculate is likely due to the reduced membrane packing under F/T conditions. Finally, to extract the content mix efficiency of the LUV compositions tested (Fig. 4E), we normalized the calcein fluorescence intensity observed in grown vesicles (Fig. 4C) by

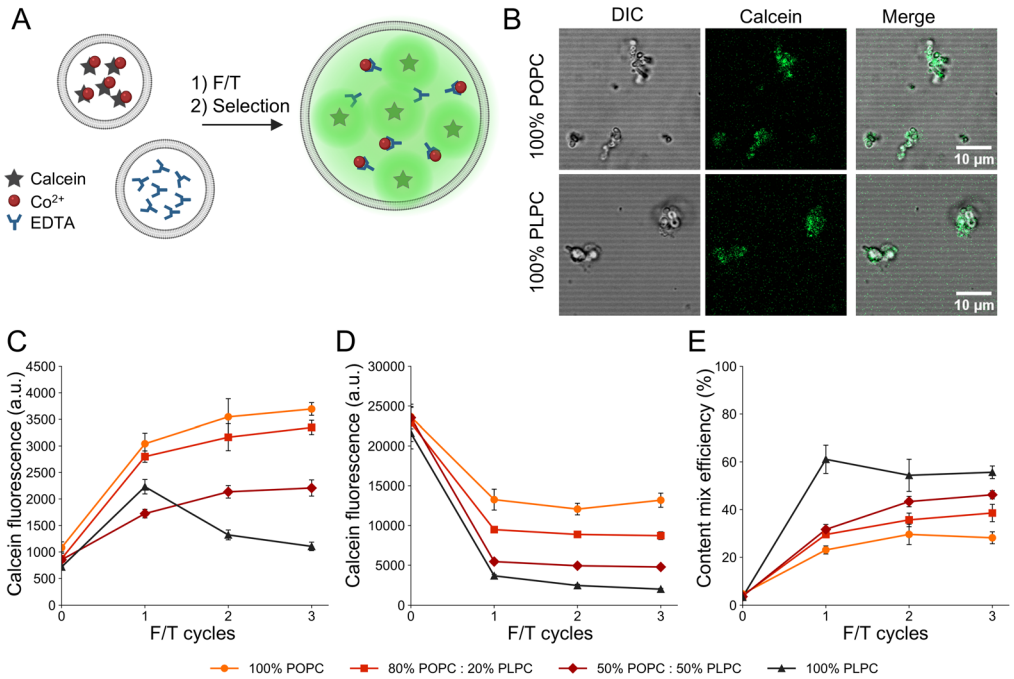

Fig. 4 Content mixing and leakage of F/T-induced grown vesicles with different phospholipid compositions. (A) Schematic of the calcein-Co^{2+}-EDTA assay for quantifying content mixing. Calcein exhibits fluorescence when Co^{2+} is removed by EDTA chelation. (B) Representative LSCM images of grown vesicles in the content mixing assay obtained by (i) DIC observation, (ii) fluorescence observation with an excitation wavelength corresponding to calcein (488 nm), and (iii) a merged image of (i) and (ii). Imaging was performed using a 63 × /1.40 oil-immersion objective lens at room temperature. (C) Calcein fluorescence in the initial LUVs (0 × F/T cycle) and in grown vesicles after 1–3 × F/T cycles. The fluorescence signals are derived from an equal amount of lipid vesicle (10 μg). (D) Calcein leakage over 1–3 × F/T cycles. Vesicles used in this experiment were prepared with an internal content consisting of a mixture of the calcein-Co^{2+} complex and EDTA at the concentrations in (C). The fluorescence signals shown are derived from an equal amount of lipid vesicle (10 μg). Therefore, these data were used as the fluorescence value representing 100% content mix efficiency for each phospholipid composition at each F/T cycle. (E) Content mix efficiencies of LUVs over 1–3 × F/T cycles calculated from data in (C) and (D). Each error bar represents the standard deviation calculated from two independent experiments, each with three measurements ($n = 6$).

subtracting the effect of content leakage (Fig. 4D, see Materials and methods in SI), and found that higher PLPC content resulted in higher content mix efficiency (Fig. 4E).

Correlation between degree of lipid unsaturation and growth fraction, membrane mix efficiency, and content mix efficiency

We have quantified the effect of phospholipid composition on the (i) F/T-induced growth fraction (Fig. 2) and the (ii) membrane mixing (Fig. 3) and (iii) content mixing efficiencies (Fig. 4) of grown vesicles by varying the ratio of POPC and PLPC. Our results showed that a higher fraction of PLPC led to not only a higher growth fraction but also a more effective mixing of membranes and contents in the grown vesicles. Given that POPC has one double bond in the acyl chains and PLPC has two double bonds, we speculated that double bonds in the phospholipid promote fusion and thus growth, membrane mixing, and content mixing. We applied the same experimental setup to LUVs consisting of DOPC, a di-monounsaturated phospholipid, which has two double bonds in total, like PLPC, but in different acyl chains (Fig. 1D). Similarly to PLPC, 100% DOPC LUVs showed a higher growth fraction, membrane mix efficiency, and content mix efficiency than POPC LUVs over 1–3 × F/T cycles (Fig. S8), indicating that one additional double bond, with relatively little dependence on its position, critically changes vesicle behavior.

We then introduced a parameter, "degree of unsaturation", to compare our assay results across various compositions based on the number of double bonds in the lipid composition. Degree of unsaturation is taken to be an average number of double bonds in the acyl chains per phospholipid comprising the initial LUVs. We found a strong positive correlation ($r > 0.9$) between the degree of unsaturation and growth fraction (Fig. 5A). The superior growth of initial LUVs with higher degree of unsaturation can be attributed to differences in the physicochemical properties of lipids such as phase transition temperatures (T_m), or the lateral packing properties of membrane.

We speculate that membrane lateral packing, rather than T_m of individual phospholipids, plays a more significant role in vesicle growth in our experimental setup. The T_m values of POPC, PLPC, and DOPC are −2 °C, −18 °C, and −17 °C, respectively.[31] Given that vesicle fusion can occur in confined spaces between ice crystals at subzero temperatures, vesicles composed of lipids with lower T_m, such as PLPC and DOPC may retain higher membrane fluidity in these confined spaces, facilitating fusion. However, vesicle confinement was already

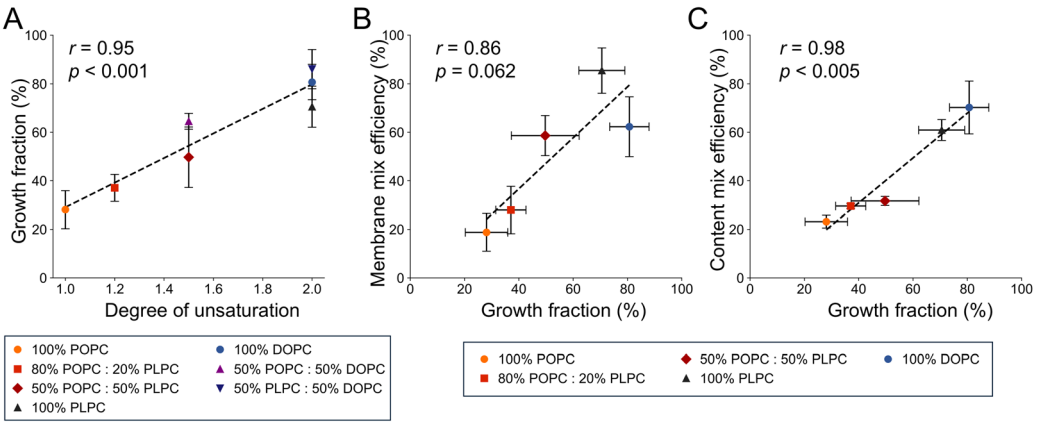

Fig. 5 Comparison of vesicle behaviors after 1 × F/T cycle among various phospholipid compositions. (A) Growth fraction as a function of "degree of unsaturation," defined as the average number of double bonds in acyl chains per phospholipid constituting the initial LUVs. Correlation of growth fraction with (B) membrane mix efficiency and (C) content mix efficiency. Each data point corresponds to different phospholipid compositions of initial LUVs as indicated in the legend. Linear regression lines are provided as visual guides to illustrate the positive trend, along with pearson correlation coefficients (r) and estimated p-values.

ensured by ultracentrifugation in our experiments, making additional ice crystal-induced confinement unlikely to play a major role. The limited influence of ice crystal confinement is further supported by the observation that the growth fraction generally exhibited small differences depending on whether the frozen sample was thawed moderately at 24 °C or rapidly at 65 °C across the three phospholipids over 1–3 × F/T cycles (Fig. S9). Therefore, we suppose that the correlation between the degree of unsaturation and growth fraction we observed is owing to membrane lateral packing. More unsaturated phospholipids like DOPC and PLPC tend to form less densely packed membranes than POPC.[32,33] Under the stresses of ice crystal formation, membranes can become destabilized or fragmented, requiring structural reorganization upon thawing. The loosely packed lateral organization due to the higher degree of unsaturation may expose more hydrophobic regions during membrane reconstruction, facilitating interactions with adjacent vesicles and making fusion energetically favorable.

Furthermore, both the membrane and content mix efficiencies exhibited positive correlation ($r > 0.85$) with growth fraction (Fig. 5B and C), suggesting that F/T-induced grown vesicles can be selectively composed of growth-prone phospholipids, and simultaneously being enriched with contents originally encapsulated in growth-prone vesicles. Taken together, these data indicate that the degree of unsaturation reports on the ease of vesicle fusion, at least for the lipids used in these experiments.

F/T cycles induced the selection of a phospholipid and accompanied enrichment of genetic molecules

Assuming LUVs consisting of POPC and PLPC coexist, grown vesicles emerging as a result of the F/T cycles may selectively contain more PLPC than POPC due to the greater growth fraction of pure PLPC vesicles compared to pure POPC vesicles (Fig. 1B). In addition, as the content of PLPC vesicles tend to be transferred more to grown vesicles compared to POPC vesicles, the preference for PLPC may also lead to the enrichment of contents initially encapsulated in PLPC vesicles (Fig. 1C).

To test this hypothesis, we first developed an analytical method to quantify POPC and PLPC from mixed fractions using high-performance liquid chromatography with evaporative light scattering detection (HPLC/ELSD) (Fig. 6A and S10). We subjected a 1 : 1 weight mixture of 100% POPC LUVs and 100% PLPC LUVs to F/T cycles. As expected, the PLPC/POPC ratio of the grown vesicles increased approximately two-fold (0.98 ± 0.07 to 1.83 ± 0.13) after 3 × F/T cycles, indicating selective incorporation of PLPC into the grown vesicles (Fig. 6B). We also investigated whether encapsulated molecules in the initial vesicle population were enriched by using DNA as a model analyte (Fig. 1C). DNA encoding green fluorescent protein (GFP-DNA, 956 bp) and mScarlet protein (mScarlet-DNA, 929 bp) were encapsulated in 100% POPC LUVs and 100% PLPC LUVs, respectively. These two LUV populations were mixed at a 1 : 1 lipid mass ratio and subjected to 1–3 × F/T cycles. DNAs encapsulated in the initial LUV mixture and the grown vesicles were recovered and subjected to quantitative PCR (qPCR). As a result, following each F/T cycle (Fig. 6C), the copy number ratio of mScarlet-DNA to GFP-DNA increased by two-fold (1.96 ± 0.15 to 4.31 ± 0.08) after 3 × F/T cycles (Fig. 6D). We find that grown vesicles that form through F/T cycles exhibited both a bias toward PLPC and preferential retention of DNA, while selectively neutral, originating from PLPC LUVs. These results demonstrate that the enrichment of compartmentalized genetic molecules in the absence of selection pressure can be driven by F/T-induced selection of membrane lipids.

Implications for primitive cellular systems under prebiotic environments

Our results of effective transfer of encapsulated contents along with growth-prone lipids indicate informational continuity between "generations" of vesicles. Here, we consider whether

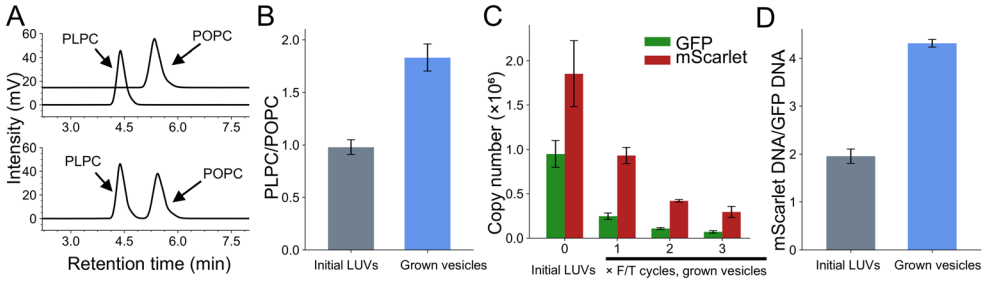

Fig. 6 Selection of membrane lipids and the coupled enrichment of encapsulated genetic molecules. (A) Representative chromatogram from HPLC/ELSD analysis of POPC and PLPC, measured separately (top) and as a 1 : 1 mass ratio mixture (bottom) (see Materials and methods and Fig. S10 in SI for details). (B) Changes in the PLPC/POPC mass ratio over F/T cycles. Data from the initial LUVs and the grown vesicles collected after 3 × F/T cycles are compared. (C) Copy numbers of GFP-DNA (green) and mScarlet-DNA (red) extracted from the initial LUV mixture and the grown vesicles obtained after 1–3 × F/T cycles. DNA was quantified by qPCR. (D) The change in mScarlet-DNA/GFP-DNA molar ratio from the initial LUVs compared to that from the grown vesicles after 3 × F/T cycles. Error bars represent the standard deviation from three independent experiments ($n = 3$).

such processes we observed using POPC and PLPC could have occurred under prebiotic environmental conditions.

We used phosphatidylcholine (PC) as membrane components, owing to their chemical structural continuity with modern cells, potential availability under prebiotic condition,[19–21] and retaining ability of essential contents. The comparison among three PC lipids highlighted that only a small difference in the acyl chain is sufficient to dramatically change the membrane behavior under F/T conditions, leading to the membrane-composition based selection. While further experiments are needed, we speculate that similar selection could occur among other amphiphilic molecules with greater chemical or structural differences, including phospholipids other than PC and fatty acids, which could have been more easily synthesized on early Earth than di-acyl chain phospholipids.[1,34]

F/T cycles in nature, driven by geological or environmental processes such as diurnal and seasonal temperature changes, or tidal-induced ice-ocean convections[30,35,36] occur much more slowly than our experimental timescales. As a consequence of such slow freezing and thawing, vesicles are expected to spend a longer time near the phase transition temperature, where membranes become destabilized and transiently permeable, which would likely enhance the mixing of encapsulated contents[37] (if the lipid Tm lies within the F/T temperature range). In addition, slow freezing can lead to the gradual growth of water ice crystals, which exclude solutes within the inter-crystal liquid phase, resulting in eutectic concentration. This concentrated environment, combined with prolonged vesicle proximity at the ice boundaries, is expected to promote vesicle fusion.[38] Moreover, eutectic concentration could facilitate the uptake of denser molecular systems. It is important to note that F/T cycles also induce contents leakage as shown in Fig. 4D. Vesicle fusion and content mixing are induced by the destabilization of the vesicle, while the same mechanism induces content release, and there is a trade-off between the two. The fusion and content exchange can occur more when vesicles are in proximity, and eutectic concentration might have played an essential role in achieving such situation. We consider ultra-centrifugation, though unrealistic in the natural settings, analogous to the eutectic concentration in vesicle–vesicle contact within a confined space.

Beside F/T cycles, dry–wet cycles have been well discussed as plausible prebiotic drivers for chemical evolution.[39,40] The drying conditions, however, may cause excessive dehydration and heat stress, leading to irreversible denaturation of molecules including proteins and lipid bilayer. We believe that F/T cycles can be an effective environment when the reaction and the molecules require water molecules. In addition to induce the supply of vesicle contents from other vesicles,[28,37,41,42] F/T conditions have been reported to be conducive to key prebiotic pathways, such as monomer synthesis, polymerization, and ligation of RNA[43–45] as well as hybridization between kilobase-sized DNA.[46] Our demonstration on how F/T cycles can directly effect vesicle behavior depending on physicochemical properties of lipid membranes additionally supports that icy conditions could have played a significant role in facilitating the selective assembly of biomolecules and molecular systems, providing a key step toward contemporary cellular systems.

Conclusions

The present study demonstrated that phospholipid composition contributes to vesicle growth under F/T cycling conditions. Furthermore, we showed that genetic molecules can be selectively enriched within the grown vesicles based on their originating lipid composition instead of their encoded information (Fig. 6). As phospholipid vesicles can harbor not only genetic but also other (proto-)biomolecules, our observation suggests that icy environments can drive the membrane-composition based mixing and enrichment of various components to offspring, resulting in an inheritance of the contents. A recursive selection of F/T-induced grown vesicles across successive generations may be realized by integrating fission mechanisms such as osmotic pressure or mechanical shear. With increasing molecular complexity, the intra-vesicular system, *i.e.*, gene-encoded function, ultimately may take over the protocellular fitness, consequently leading to the emergence of a primordial cell capable of Darwinian evolution.

Author contributions

TS performed most of the experiments, TW established the experimental protocol for ELSD measurement. TS, KK, YS, TM conceived the project, TS, NN and TM wrote the paper, and all authors discussed the project and edited the manuscript. We thank Tony Z. Jia and Liam M. Longo (ELSI, Institute of Science Tokyo) for the critical reading of the manuscript and many constructive comments, and Prof. Yoshikazu Tanaka (Tohoku University) for TEM analysis of the vesicles at the early phase of the project.

Conflicts of interest

There are no conflicts to declare.

Data availability

The source data generated for Fig. 2–6 and S1–S10 (in supplementary information (SI)) are available for download from the open access repository at **https://doi.org/10.6084/m9.figshare.29401220.v3**. Supplementary information is available. See DOI: **https://doi.org/10.1039/d5sc04710b**.

Acknowledgements

This study was supported by the Human Frontier Science Program Grant Number RGP003/2023 (TM), JSPS KAKENHI Grant Numbers 22KJ1296 (NN), 22K21344 (TM), and 21H05228 (TM), JST SPRING, Grant Number JPMJSP2180 (TS), and the Astrobiology Center Program of the National Institutes of Natural Sciences (NINS) Grant Number JY230122nn (TM).

References

1 S. Sarkar, S. Das, S. Dagar, M. P. Joshi, C. V. Mungi, A. A. Sawant, G. M. Patki and S. Rajamani, *J. Membr. Biol.*, 2020, **253**, 589–608.
2 R. Mizuuchi and N. Ichihashi, *Life*, 2021, **11**, 191.
3 J. W. Szostak, D. P. Bartel and P. L. Luisi, *Nature*, 2001, **409**, 387–390.
4 I. A. Chen, R. W. Roberts and J. W. Szostak, *Science*, 2004, **305**, 1474–1476.
5 K. Adamala and J. W. Szostak, *Nat. Chem.*, 2013, **5**, 495–501.
6 H. Lu, A. Blokhuis, R. Turk-MacLeod, J. Karuppusamy, A. Franconi, G. Woronoff, C. Jeancolas, A. Abrishamkar, E. Loire, F. Ferrage, P. Pelupessy, L. Jullien, E. Szathmary, P. Nghe and A. D. Griffiths, *Nat. Chem.*, 2024, **16**, 70–78.
7 D. Segré, D. Ben-Eli, D. W. Deamer and D. Lancet, *Orig. Life Evol. Biosph.*, 2001, **31**, 119–145.
8 D. Segré, D. Ben-Eli and D. Lancet, *Proc. Natl. Acad. Sci. U. S. A.*, 2000, **97**, 4112–4117.
9 O. Markovitch and D. Lancet, *J. Theor. Biol.*, 2014, **357**, 26–34.
10 D. Lancet, R. Zidovetzki and O. Markovitch, *J. R. Soc. Interface*, 2018, **15**, 20180159.
11 J. M. P. Gutierrez, T. Hinkley, J. W. Taylor, K. Yanev and L. Cronin, *Nat. Commun.*, 2014, **5**, 5571.
12 Z. Cheng and P. L. Luisi, *J. Phys. Chem. B*, 2003, **107**, 10940–10945.
13 I. Budin and J. W. Szostak, *Proc. Natl. Acad. Sci. U. S. A.*, 2011, **108**, 5249–5254.
14 P. Dalai, P. Ustriyana and N. Sahai, *Geochim. Cosmochim. Acta*, 2018, **223**, 216–228.
15 K. Ruiz-Mirazo, C. Briones and A. de la Escosura, *Chem. Rev.*, 2014, **114**, 285–366.
16 J. Gutknecht, *J. Membr. Biol.*, 1988, **106**, 83–93.
17 X. Zhou, P. Dalai and N. Sahai, *Life*, 2020, **10**, 39.
18 A. C. Chakrabarti and D. W. Deamer b, *Biochim. Biophys. Acta*, 1992, **1111**, 171–177.
19 W. R. Hargreaves, S. J. Mulvihill and D. W. Deamer, *Nature*, 1977, **266**, 78–80.
20 C. Bonfio, C. Caumes, C. D. Duffy, B. H. Patel, C. Percivalle, M. Tsanakopoulou and J. D. Sutherland, *J. Am. Chem. Soc.*, 2019, **141**, 3934–3939.
21 L. Liu, Y. Zou, A. Bhattacharya, D. Zhang, S. Q. Lang, K. N. Houk and N. K. Devaraj, *Nat. Chem.*, 2020, **12**, 1029–1034.
22 I. Ivanov, R. B. Lira, T.-Y. D. Tang, T. Franzmann, A. Klosin, L. C. da Silva, A. Hyman, K. Landfester, R. Lipowsky, K. Sundmacher and R. Dimova, *Adv. Biosyst.*, 2019, **3**, e1800314.
23 N. Berclaz, M. Müller, P. Walde and P. L. Luisi, *J. Phys. Chem. B*, 2001, **105**, 1056–1064.
24 M. M. Hanczyc, S. M. Fujikawa and J. W. Szostak, *Science*, 2003, **302**, 618–622.
25 H. Ellens, J. Bentz and F. C. Szoka, *Biochemistry*, 1985, **24**, 3099–3106.
26 T. D. Ingolia and D. E. Koshland Jr, *J. Biol. Chem.*, 1978, **253**, 3821–3829.
27 J. Chen, L. Tanwar, P. Ji, R. J. Brea and N. K. Devaraj, *ChemSystemsChem*, 2025, **7**(3), e202400077.
28 G. Tsuji, S. Fujii, T. Sunami and T. Yomo, *Proc. Natl. Acad. Sci. U. S. A.*, 2016, **113**, 590–595.
29 K. Zahnle, N. Arndt, C. Cockell, A. Halliday, E. Nisbet, F. Selsis and N. H. Sleep, *Space Sci. Rev.*, 2007, **129**, 35–78.
30 M. G. Fox-Powell and C. R. Cousins, *J. Geophys. Res. Planets*, 2021, **126**, e2020JE006628.
31 M. R. Morrow, P. J. Davis, C. S. Jackman and K. M. Keough, *Biophys. J.*, 1996, **71**, 3207–3214.
32 S. Vanni, H. Hirose, H. Barelli, B. Antonny and R. Gautier, *Nat. Commun.*, 2014, **5**, 4916.
33 R. Ernst, C. S. Ejsing and B. Antonny, *J. Mol. Biol.*, 2016, **428**, 4776–4791.
34 D. Deamer, J. P. Dworkin, S. A. Sandford, M. P. Bernstein and L. J. Allamandola, *Astrobiology*, 2002, **2**, 371–381.
35 F. Postberg, N. Khawaja, B. Abel, G. Choblet, C. R. Glein, M. S. Gudipati, B. L. Henderson, H.-W. Hsu, S. Kempf, F. Klenner, G. Moragas-Klostermeyer, B. Magee, L. Nölle, M. Perry, R. Reviol, J. Schmidt, R. Srama, F. Stolz, G. Tobie, M. Trieloff and J. H. Waite, *Nature*, 2018, **558**, 564–568.
36 T. H. Vu, M. Choukroun, R. Hodyss and P. V. Johnson, *Icarus*, 2020, **349**, 113746.
37 B. Peter and P. Schwille, *ChemSystemsChem*, 2023, **5**(5), e202300008.

38 A. P. Costa, X. Xu and D. J. Burgess, *Pharm. Res.*, 2014, **31**, 97–103.
39 B. Damer and D. Deamer, *Life*, 2015, **5**, 872–887.
40 B. Damer and D. Deamer, *Astrobiology*, 2020, **20**, 429–452.
41 T. Litschel, K. A. Ganzinger, T. Movinkel, M. Heymann, T. Robinson, H. Mutschler and P. Schwille, *New J. Phys.*, 2018, **20**, 055008.
42 E. Salibi, B. Peter, P. Schwille and H. Mutschler, *Nat. Commun.*, 2023, **14**, 1222.
43 C. Menor-Salván, D. M. Ruiz-Bermejo, M. I. Guzmán, S. Osuna-Esteban and S. Veintemillas-Verdaguer, *Chemistry*, 2009, **15**, 4411–4418.
44 S. J. Zhang, D. Duzdevich, D. Ding and J. W. Szostak, *Proc. Natl. Acad. Sci. U. S. A.*, 2022, **119**, e2116429119.
45 H. Mutschler, A. Wochner and P. Holliger, *Nat. Chem.*, 2015, **7**, 502–508.
46 N. Noda, K. Nomura, N. Takahashi, F. Hashiya, H. Abe and T. Matsuura, *ChemSystemsChem*, 2024, **6**(4), e202400025.